Electronic Supplementary Material (ESI) for Analyst.

Supporting Information

Tip-Enhanced Raman Spectroscopy of Amyloid β at Neuronal Spines

Mohammadali Tabatabaei, [†] *Fabiana A. Caetano,* [‡] *Farshid Pashaee,* [†] *Stephen S. G. Ferguson,* [‡,§] *François Lagugné-Labarthet* [†,*]

†Department of Chemistry and Center for Advanced Materials and Biomaterials, University of Western Ontario, London, ON, Canada N6A 5B7

‡ Department of Physiology and Pharmacology, University of Western Ontario, London, Ontario, Canada N6A 5C1

§ Department of Cellular and Molecular Medicine, University of Ottawa, Ottawa, ON, Canada K1H 8M5

AUTHOR INFORMATION

Corresponding Author

*E-mail: flagugne@uwo.ca; Tel.: +1 519 661 2111×81006; Fax: +1 519 661 3022

TERS setup and tip preparation. The TERS setup combines a Raman spectrometer (HR LabRam, Horiba) and an inverted optical microscope (Olympus IX71) and is interfaced with a 5 axis AFM instrument (NanoWizard II equipped with a TAO stage, JPK Instruments Inc.). The three axis (x, y, z) piezo-actuator of the cantilever allows for the precise positioning of the tip within the center of the focal point. In this geometry, light is focused from below via the glass coverslip onto the tip and the sample. The tip is in feedback with the sample and interacts at the focal point with the evanescent waves confined at the surface of the sample. An oil immersion objective with a N.A. of 1.4 and ×100 magnification (PlanAPO Olympus) was used for focusing the excitation laser on the sample and for collection of the Raman signal in backscattering configuration. Raman-scattered photons were detected using a liquid nitrogen cooled CCD camera (Horiba, Symphony). A grating of 600 grooves per mm together with an 800 mm spectrometer focal length yielded a spectral resolution of ~1.5 cm^{-1}. The intensities of the linearly polarized excitation laser (He-Ne laser, λ= 632.8 nm) were around 600 μW. The size of the beam was adjusted to fill the entrance pupil of the objective. TERS signals were collected with 20 s acquisition time. TERS mappings were collected with 5 s acquisition time with the step size of 100 nm. Spectra were acquired in the [800-3200] cm^{-1} spectral range. The band centered at 970 cm^{-1} is the second order scattering from the phonon mode of silicon that compose the bulk of the TERS tip used for this study (Fig. 2A and Fig.3). Even though the tip is coated with a gold layer, the scattering from bulk silicon of the tip is yet intense. The intensity of the second order scattering of Si was used to

normalize our TERS spectra and generate the associated maps. The background correction based on a polynomial fit has been applied to the all spectra and for the mappings, unless mentioned. The TERS maps were corrected considering the Raman intensities associated with the neuronal projection's membrane. The AFM tip used for these experiments was prepared from commercially available silicon cantilever (NCL50, NANO WORLD Innovative Technologies, f = 190 kHz, k = 48 N m^{-1}). These tips have been coated with a 5 nm of Ti as an adhesion layer followed by 30 nm of gold using electron-beam evaporation. TERS tips were further annealed for 30 min at 180°C to generate more uniform gold islands at the apex of the TERS tip.

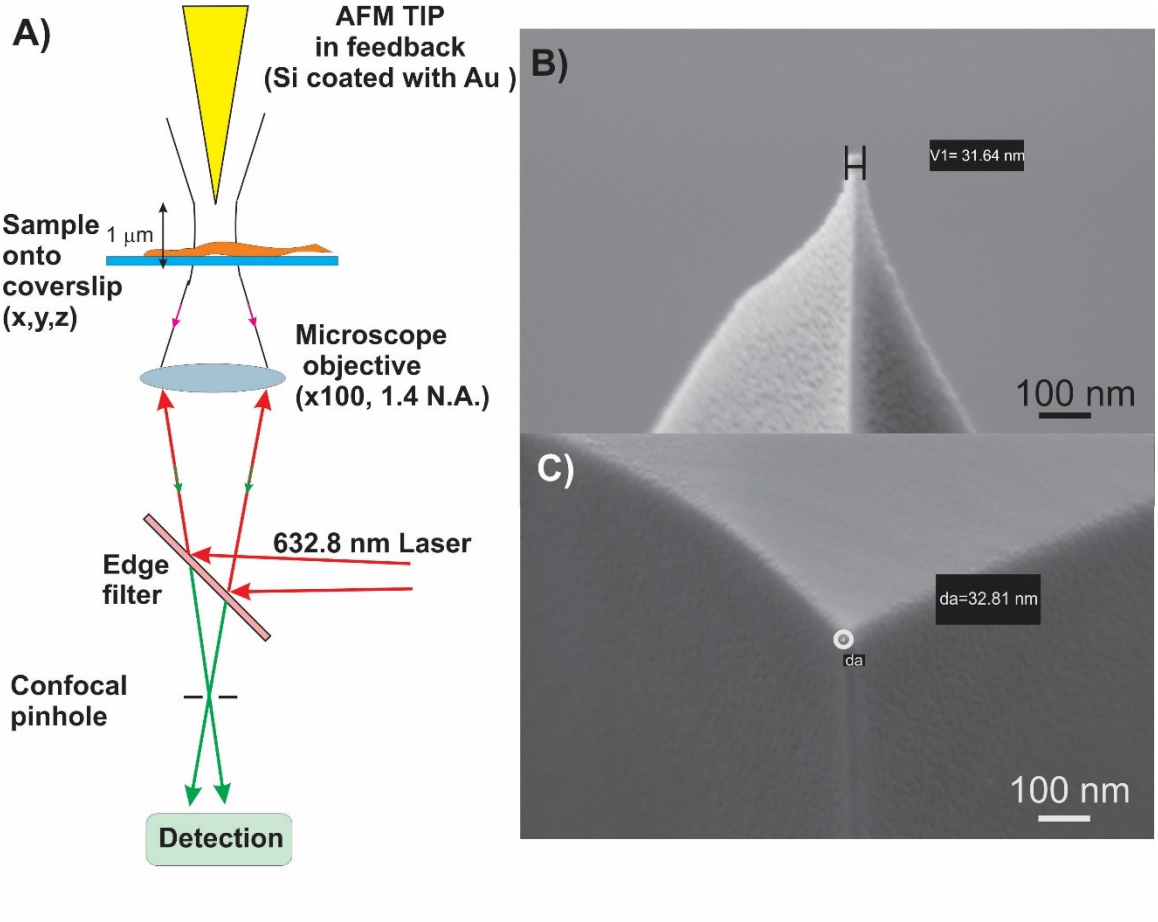

Figure S1. (A) Schematics of the TERS setup. (B, C) Side view and top view SEM images of the coated silicon tip with 5 nm of titanium and 30 nm of gold.

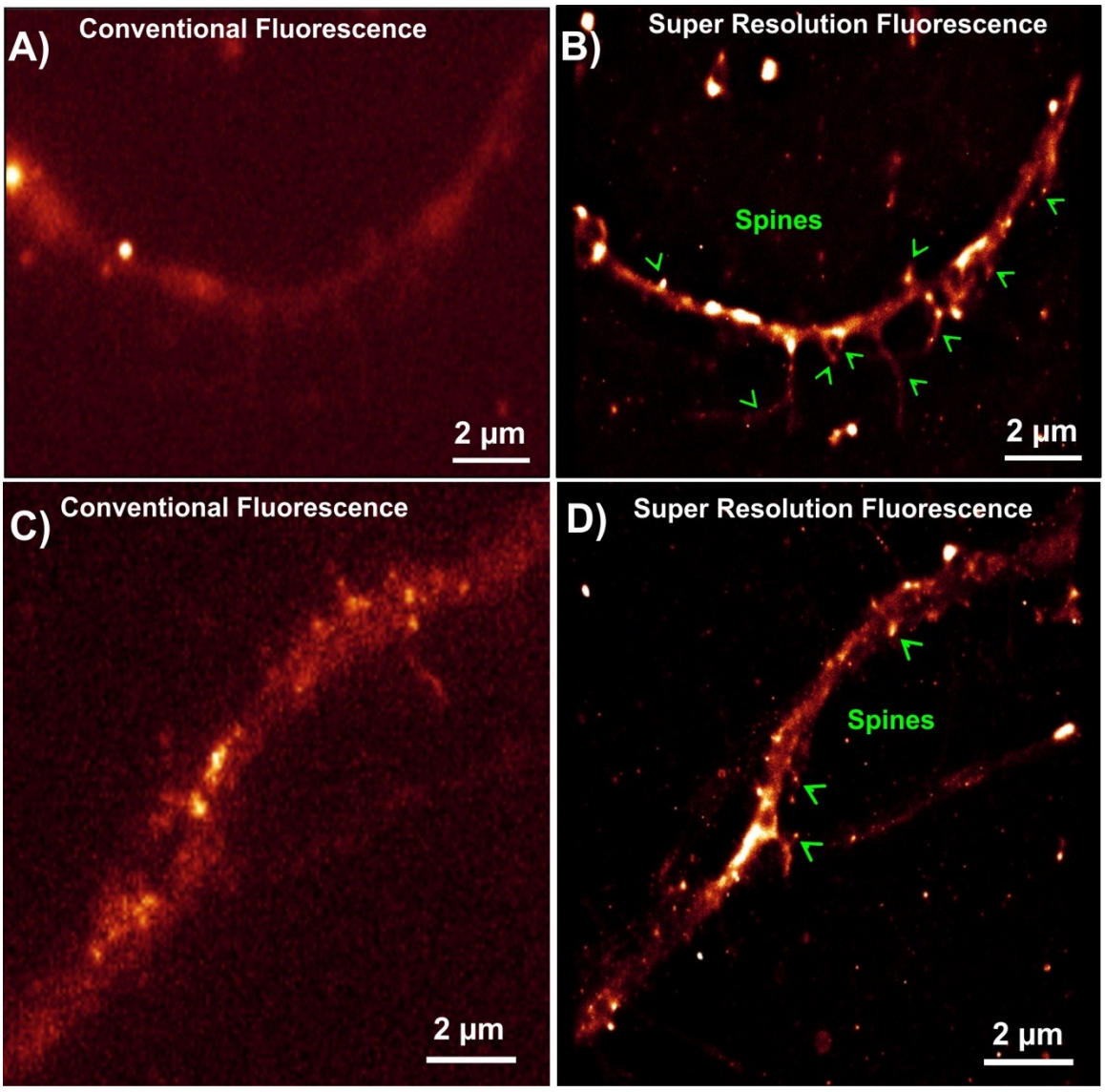

Figure S2. Calcein-immunostained fluorescence images of hippocampal neurons obtained by conventional wide-field epi-fluorescence (A and C) and GSD-super resolution fluorescence (B and D) microscopies. Spines localizations have been shown by arrows in super resolution images in B and D.

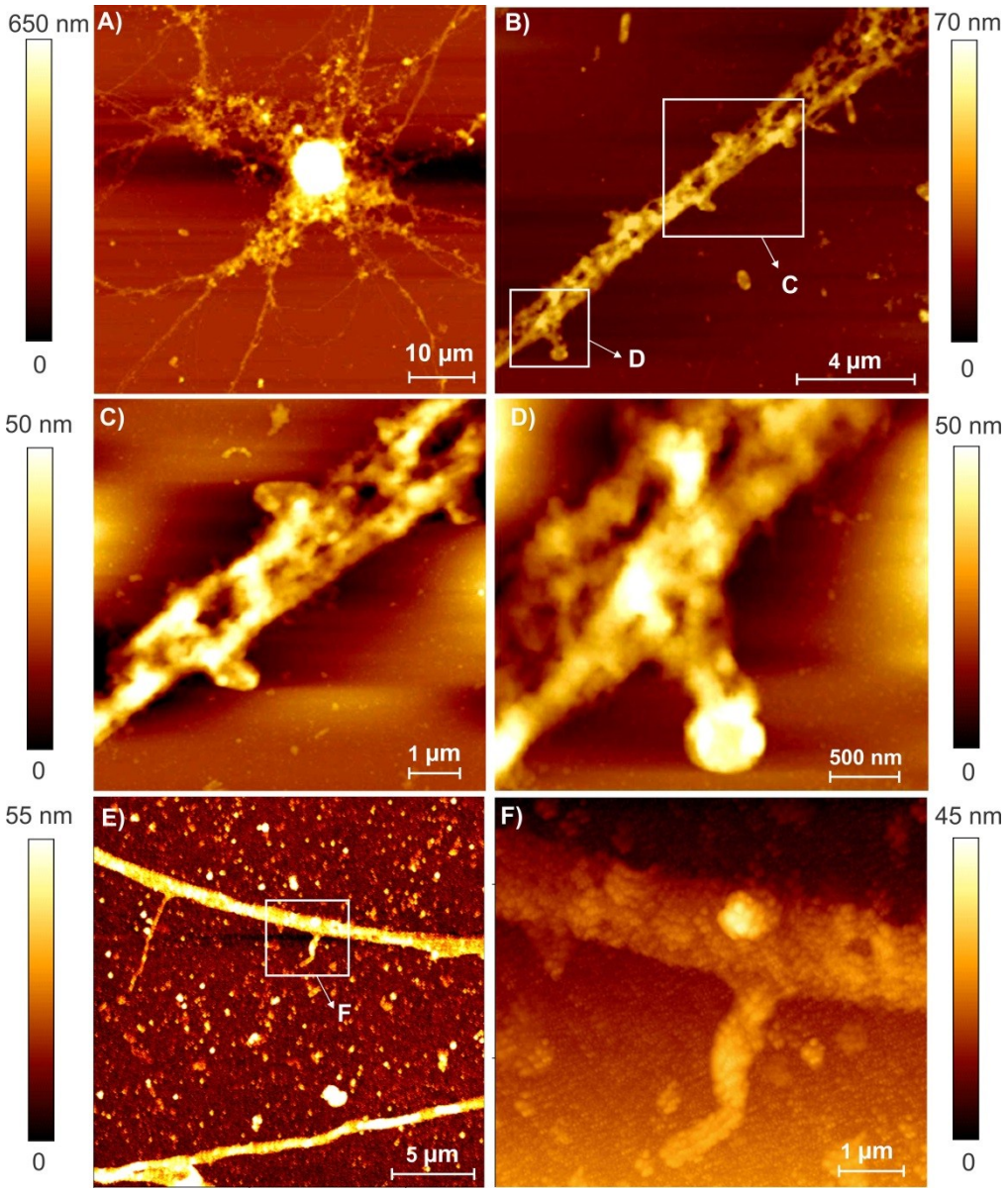

Figure S3. AFM images of non-treated neuronal projections and spines of hippocampal neurons. A) AFM morphology of a neuronal nucleus and projections. B) AFM morphology of neuronal projections and spines. C,D) selected regions on B, demonstrating the localization of projected spines out of the projections. E,F) neuronal projection and spines of another non-treated area.

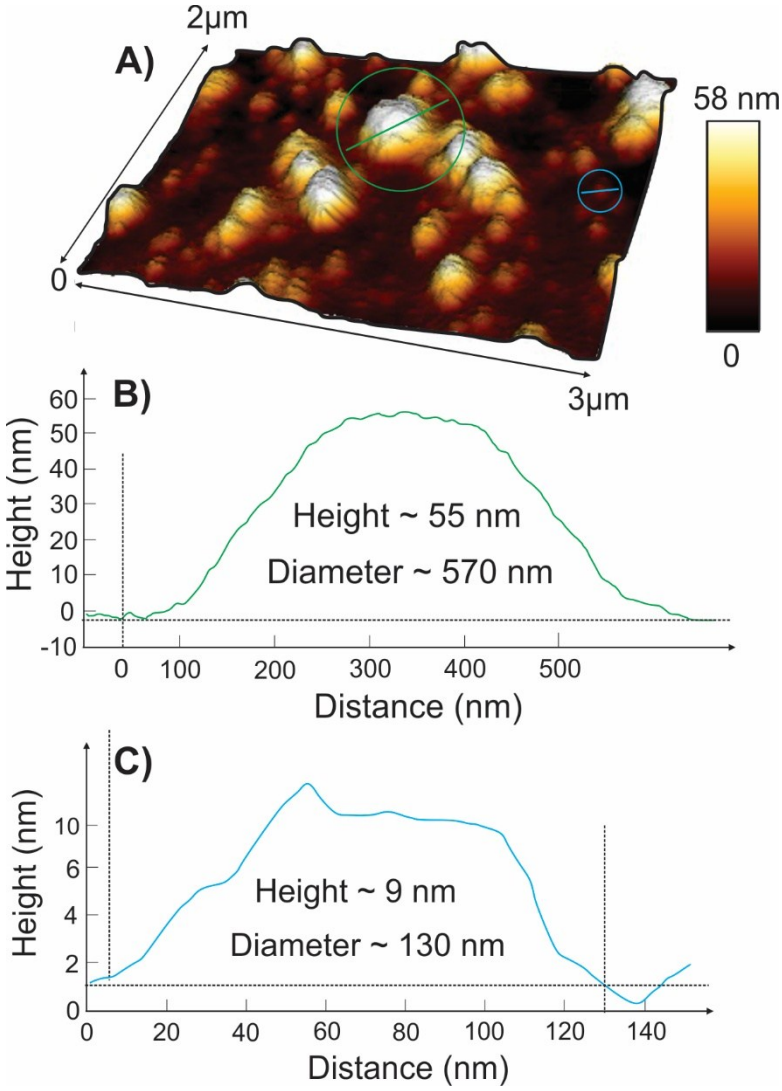

Figure S4. AFM of Aβ plaques grown on mica. A) AFM topography of plaque structures formed by Aβ oligomers; B) cross-section of the selected region in green; C) cross-section of the selected region in blue.

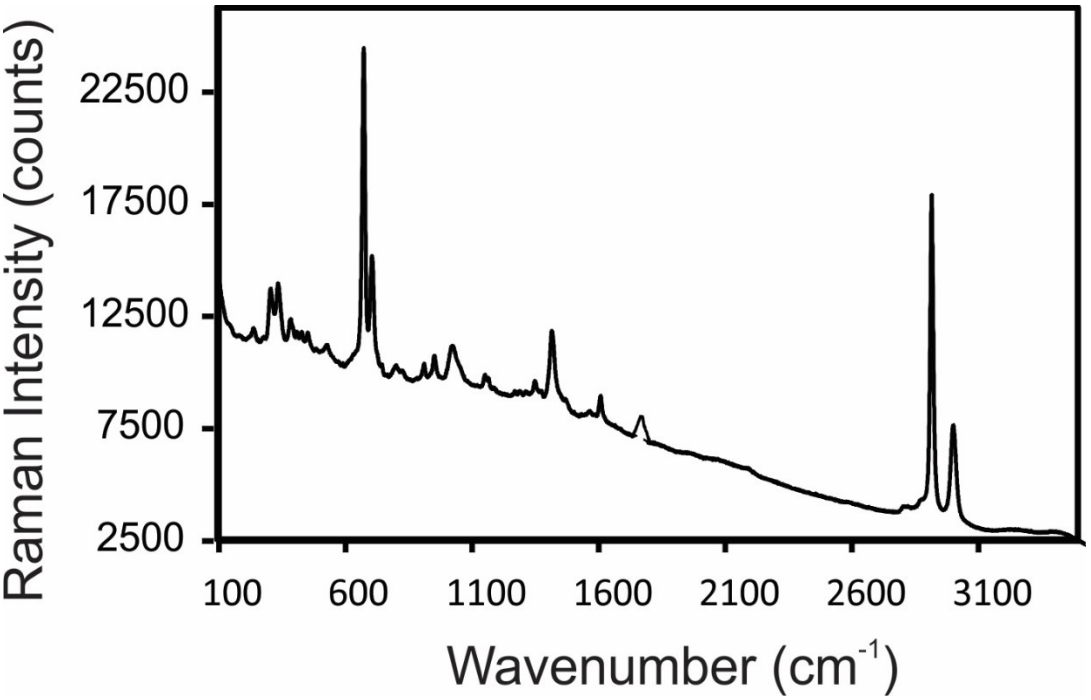

Figure S5. Confocal Raman spectra acquired on the sample shown in Fig S2. The Raman bands assignment is reported in Table S1.

Table S1. Extracellular Aβ plaques Raman assignement [1-12]

Raman Shift (cm^{-1})	Assignment	Ref
672	Tyr, Cys	1, 2
716	Glu, Asn, Thr	2, 3
829	Tyr	3-5
913		
955	Lys	3, 5
1004	Phe	2-6
1030	Phe	5, 7, 8
1151	Phe, Ile	5, 7, 9
1240-1350	Amide III	1, 5, 7, 10, 11
1450	Ala, Val, Leu, Lys	2, 3, 5, 7
1606	Phe, Tyr^{-}	3, 5, 7, 12

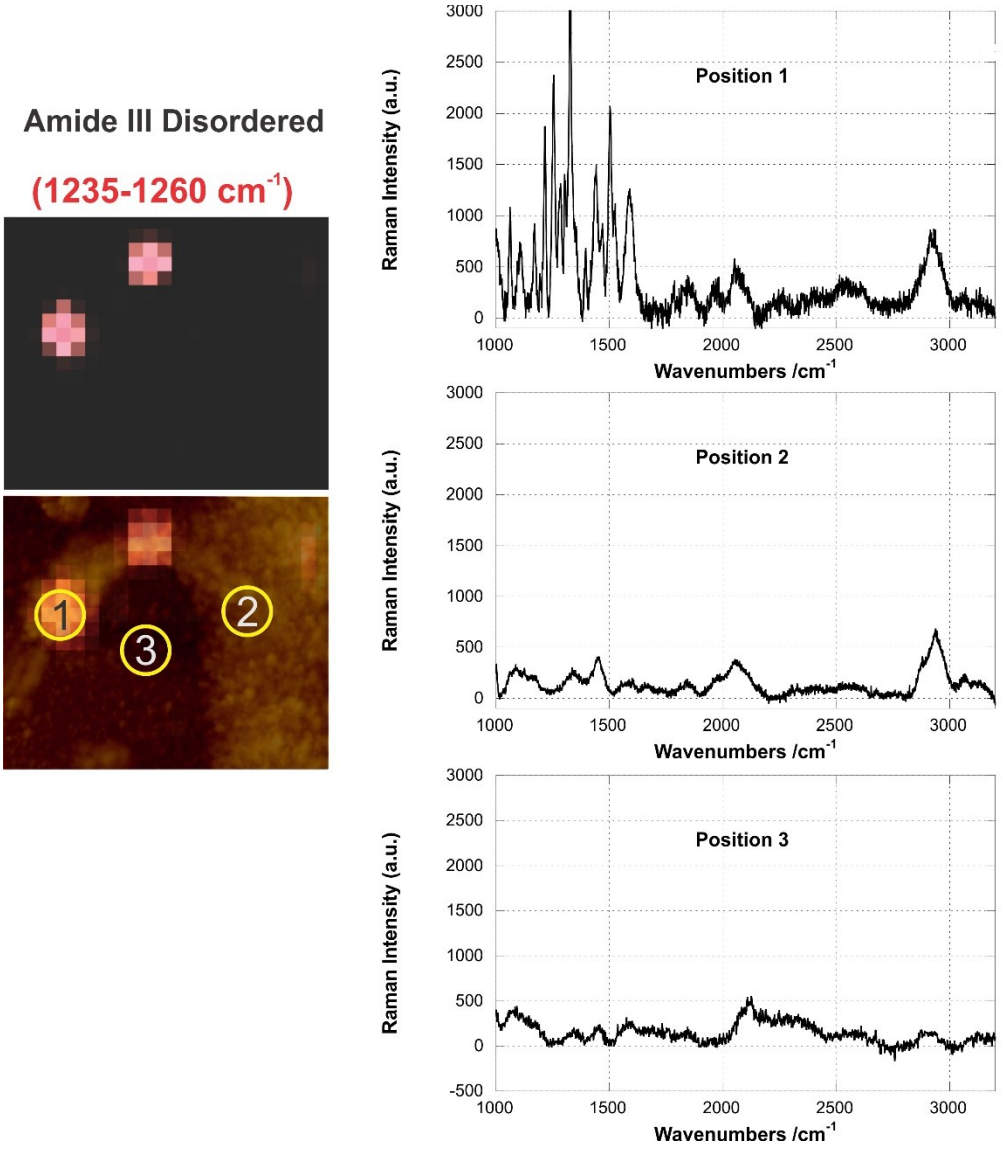

Figure S6. TERS spectra of selected areas on neuronal projections. The spectra were normalized with respect to the Silicon signal and background corrected.

Comparison of TERS spectra collected in the vicinity of the projection using the same intensity scale. In areas where amyloid-β aggregates are located (position 1), vibrational markers with strong intensity clearly appear between 1000 and 1800 cm^{-1}. Weak signal is present for area of the projection where no amyloid beta is present (position 2). The C-H stretching region is clearly visible for both region 1 and 2 with similar intensity. This

spectral region is mostly assigned to the signal of the membrane. No Confocal Raman (with TERS tip out) could be recorded in these areas. The TERS background corresponding to the substrate is shown for position 3 for sake of comparison. The CH stretching region is absent in position 3.

References

(1) Chou, I. H.; Benford, M.; Beier, H. T.; Coté, G. L.; Wang, M.; Jing, N.; Kameoka, J.; Good, T. A. *Nano Lett.* **2008**, *8*, 1729-1735.

(2) Deckert-Gaudig, T.; Kämmer, E.; Deckert, V. *J. Biophotonics* **2012**, *5*, 215-219.

(3) Stewart, S.; Fredericks, P. M. *Spectrochim. Acta A* **1999**, *55*, 1641-1660.

(4) Guicheteau, J.; Argue, L.; Hyre, A.; Jacobson, M.; Christesen, S. D. In *Proc. SPIE*, 2006, pp 62180O-62180O-62111.

(5) Paulite, M.; Blum, C.; Schmid, T.; Opilik, L.; Eyer, K.; Walker, G. C.; Zenobi, R. *ACS Nano* **2013**, *7*, 911-920.

(6) Tabatabaei, M.; Wallace, G. Q.; Caetano, F. A.; Gillies, E. R.; Ferguson, S. S. G.; Lagugné-Labarthet, F. *Chem. Sci.* **2016**, *7*, 575-582.

(7) Dong, J.; Atwood, C. S.; Anderson, V. E.; Siedlak, S. L.; Smith, M. A.; Perry, G.; Carey, P. R. *Biochemistry* **2003**, *42*, 2768-2773.

(8) Herne, T. M.; Ahern, A.; Garrell, R. L. *J. Am. Chem. Soc.* **1991**, *113*, 846-854.

(9) Kim, S. K.; Kim, M. S.; Suh, S. W. *J. Raman Spectrosc.* **1987**, *18*, 171-175.

(10) Huang, C.-Y.; Balakrishnan, G.; Spiro, T. G. *J. Raman Spectrosc.* **2006**, *37*, 277-282.

(11) Bandekar, J. *Biochim. Biophys. Acta* **1992**, *1120*, 123-143.

(12) Podstawka, E.; Ozaki, Y.; Proniewicz, L. M. *Appl. Spectrosc.* **2004**, *58*, 570-580.